

# UC Davis

## UC Davis Previously Published Works

### Title

Large Magnetoresistance and Finite-Size Effects in Electrodeposited Single-Crystal Bi Thin Films

### Permalink

<https://escholarship.org/uc/item/71473535>

### Journal

Physical Review Letters, 82(16)

### ISSN

0031-9007

### Authors

Yang, FY  
Liu, Kai  
Chien, CL  
[et al.](#)

### Publication Date

1999-04-19

### DOI

10.1103/physrevlett.82.3328

Peer reviewed

## Large Magnetoresistance and Finite-Size Effects in Electrodeposited Single-Crystal Bi Thin Films

F. Y. Yang,<sup>1</sup> Kai Liu,<sup>1</sup> C. L. Chien,<sup>1</sup> and P. C. Searson<sup>2</sup>

<sup>1</sup>*Department of Physics and Astronomy, The Johns Hopkins University, Baltimore, Maryland 21218*

<sup>2</sup>*Department of Materials Science and Engineering, The Johns Hopkins University, Baltimore, Maryland 21218*  
(Received 10 November 1998)

Trigonal-axis oriented single-crystal Bi thin films have been made by electrodeposition followed by suitable annealing. Very large magnetoresistance with ratios as much as 1500 at 5 K and 2.9 at 300 K under 5 T, Shubnikov-de Haas oscillations, and finite-size effects have been observed. [S0031-9007(99)08947-4]

PACS numbers: 73.50.Jt, 61.10.Nz, 72.15.Lh, 81.15.-z

Magnetic nanostructures, such as multilayers (e.g., Co/Cu) [1–3] and granular solids (e.g., Co-Ag) [4,5] have attracted a great deal of attention, because of the realization of negative giant magnetoresistance (GMR) due to spin-dependent scattering [6]. The largest GMR value ever reported has been about 150% at 4.2 K [7] and 80% at room temperature [8]. Most reported GMR values, particularly those in spin-valve devices, are much smaller, in the range of 10% at room temperature. Certain suitably doped manganese perovskites, due to an insulator-metal transition, exhibit negative colossal magnetoresistance (CMR) [9,10]. However, the large effect size of CMR occurs predominantly at low temperatures. At room temperature, the CMR effect is small, precluding most practical applications. In both GMR and CMR materials, the negative magnetoresistance (MR) saturates at a magnetic field of several tesla (T), and the field dependence is too complex to be useful as wide-range field sensing devices. Since both GMR and CMR involve magnetic materials, the MR is hysteretic.

Bismuth (Bi) is a semimetallic element with unusual transport properties. The electronic properties of Bi, diametrically different from those of common metals, are due to its highly anisotropic Fermi surface, low carrier densities, small carrier effective masses, and long carrier mean free path. The elongated Fermi surfaces of holes and electrons with small effective masses lead to a large Fermi wavelength  $\lambda_F$  of about 400 Å, as opposed to a few Å in most metals [11]. The carrier mean free path in Bi can be as much as a millimeter at 4.2 K, several orders of magnitude larger than those in most metals [12]. Because of these large characteristic lengths, Bi has been extensively pursued for the studies of quantum transport and finite-size effects. For example, there is a continuing pursuit of the semimetal to semiconductor transition for very thin Bi films [13–15]. Bulk single crystals of Bi are also known to exhibit a very large magnetoresistance effect [16,17].

However, the availability of high quality Bi thin films has been a major hindrance for these pursuits. The fabrication of high quality Bi thin films has been well

documented to be difficult. Bi thin films made by traditional vapor deposition methods, such as sputtering and evaporation, are polycrystalline with small grains [18,19], which often exhibit small mean free paths with disappointingly small MR effects and are undesirable for finite-size studies. Only recently has the method of molecular beam epitaxy (MBE) been able to fabricate high quality Bi films on BaF<sub>2</sub> substrates [20]. Very recently, we have demonstrated electrodeposition as an effective technique to fabricate high quality Bi nanowires in polycarbonate nanopore templates with large MR values [21,22]. In this work, we report on single-crystal Bi thin films made by electrodeposition followed by suitable annealing. These high quality trigonal-axis oriented Bi thin films exhibit very large MR, with MR ratios as much as 1500 times at low temperature and 2.9 times at room temperature. Finite-size effects and Shubnikov-de Haas oscillations have also been observed. The single-crystal Bi thin films made by electrodeposition are attractive for studying the unusual transport properties of Bi as well as for the exploration of technological applications.

The Bi thin films, 1–10  $\mu\text{m}$  thick, have been electrodeposited from a solution of bismuth nitrate pentahydrate [21]. A thin Au layer ( $\sim 100$  Å) was first sputtered onto a Si (100) wafer with a native SiO<sub>2</sub> layer. It was subsequently patterned and used as the working electrode in a three-electrode electrodeposition cell. The other two electrodes are the Pt counter electrode and the Ag<sup>+</sup>/AgCl reference electrode. The deposition rate is about 0.2  $\mu\text{m}/\text{min}$ . Some of the electrodeposited Bi films, 1 to 10  $\mu\text{m}$  thick, have been subsequently annealed in Ar at a suitable temperature for the formation of single crystals.

The x-ray diffraction pattern of an electrodeposited 5- $\mu\text{m}$  thick Bi film is shown in Fig. 1a. The as-deposited film is polycrystalline, exhibiting a large number of diffraction lines due to the rhombohedral structure of Bi. The diffraction pattern of the same film after annealing at 268 °C for 6 hours is shown in Fig. 1b, which exhibits only the (003), (006), and (009) peaks, demonstrating that the

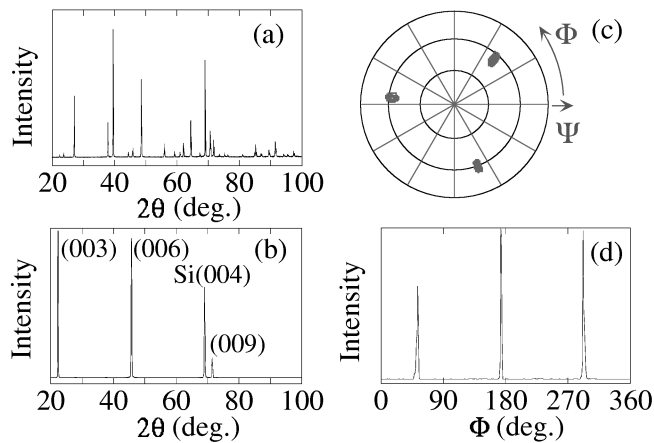


FIG. 1. X-ray diffraction patterns of a 5- $\mu\text{m}$  (a) as-electrodeposited and (b) annealed Bi film. (c) The pole figure and (d) the 57.5° tilt  $\Phi$  scan of the (012) diffraction from the annealed Bi film demonstrate its single-crystalline nature.

Bi film is exclusively trigonal-axis oriented. Pole-figure measurements show that the (012), (116), and (202) peaks have, respectively, threefold, sixfold, and threefold symmetry, of which the result for (012) is shown in Fig. 1c. A  $\Phi$  scan about the Bi (012) peak is shown in Fig. 1d, where three peaks separated by 120° are observed. These x-ray diffraction results thus conclusively demonstrate that the as-deposited polycrystalline Bi thin films, after suitable annealing, become large single-crystalline trigonal-axis oriented Bi films.

We have used a conventional four-probe method to measure the MR of the Bi films of various thicknesses in a magnetic field ( $\mathbf{B}$ ) up to 5 T. The lateral dimensions of the samples are about 6 mm  $\times$  2 mm with the current in the long direction. The MR has been measured in three geometries: perpendicular (P), longitudinal (L), and transverse (T), where  $\mathbf{B}$  is, respectively, perpendicular to the film plane, parallel to the current, and in the film plane but perpendicular to the current. Representative MR results of the as-deposited polycrystalline and the annealed single-crystalline 10- $\mu\text{m}$  Bi films at 5 and 300 K are shown in Fig. 2. Because of the very large MR effect, here we use MR ratio  $[R(\mathbf{B}) - R(\mathbf{B} = 0)]/R(\mathbf{B} = 0)$  instead of percent. For example, a MR ratio of 1530 means 153 000%. The overall sizes of the MR at 5 K of various films are shown in Table I.

The magnitude of the MR depends greatly on the quality of the sample, and, not coincidentally, on the fabrication method. For example, Bi films made by sputtering exhibit a very small MR, as small as 1% at 300 K under a 5 T field. In contrast, the as-deposited Bi films exhibit huge MR effects, with a MR ratio for the 10- $\mu\text{m}$  film of 21.4 at 5 K and 2.4 at 300 K under 5 T. The already very large MR effects in polycrystalline Bi films become even larger in the single-crystalline films. The MR ratio of the 10- $\mu\text{m}$  film increases from 21.4 to 1530, illustrating that the MR in Bi depends very

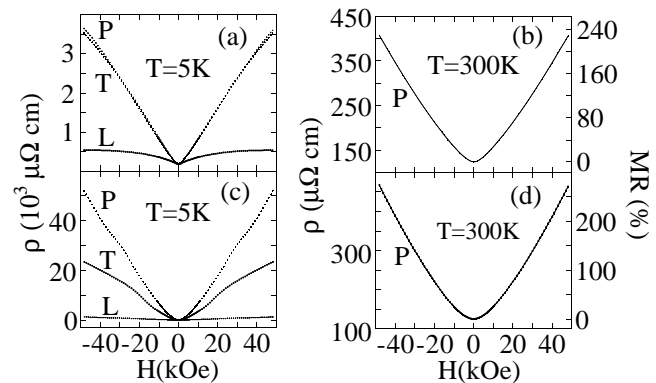


FIG. 2. Magnetoresistance results of a 10- $\mu\text{m}$  electro-deposited Bi film: (a) As-deposited polycrystalline film at 5 K in the perpendicular (P), transverse (T), and longitudinal (L) geometries; (b) as-deposited film at 300 K in the P geometry; (c) annealed single-crystalline film at 5 K in the P, T, and L geometries; (d) annealed film at 300 K in the P geometry.

sensitively on the quality of materials. The MR ratios of the single-crystalline films are similar to those grown by MBE. For example, for the thickest epitaxial Bi film of 2  $\mu\text{m}$  grown by MBE [20], the MR ratio at 5 T is about 400 at 4.2 K, essentially the same as our value of 381 at 5 T and 5 K. The MR values of the as-deposited and the annealed Bi films are much larger than the GMR in magnetic nanostructures.

From Fig. 2 and Table I, the MR in Bi films exhibits certain characteristics. The field dependence of MR is generally quasilinear except at small fields, where it is quadratic. The MR effect is nonhysteretic, i.e., the same results for both increasing and decreasing fields. The MR effect not only depends on the sample quality (through the carrier mean free path  $l$  and relaxation time  $\tau$ ) but also on the measuring geometry (P, L, or T), the thickness ( $t$ ) of the thin film due to the finite-size effects, and the temperature. The perpendicular MR is always the largest and the longitudinal MR is always the smallest. The

TABLE I. Resistivity at zero field, longitudinal (L), transverse (T), and perpendicular (P) magnetoresistance (MR) ratios of polycrystalline and single-crystalline Bi films of various thicknesses at 5 K.

Thickness ( $\mu\text{m}$ )	Resistivity ( $\mu\Omega\text{ cm}$ )	MR ratio		
		L	T	P
Polycrystalline				
10	183	2.0	21.3	21.4
5	265	2.0	17.0	19.5
2	281	1.4	3.3	3.7
1	425	1.0	2.8	3.5
Single crystalline				
10	34	35	690	1530
5	48	30	292	1080
2	65	13	84	381
1	78	8	33	234

MR ratio decreases with decreasing film thickness and increasing temperature.

In Bi, one observes the ordinary positive MR, due to the curving of carrier trajectory by the Lorentz force. Under a magnetic field  $\mathbf{B}$ , the carriers move in cyclotron orbits perpendicular to  $\mathbf{B}$  with a radius of  $r_c = m^*v/eB$ , where  $m^*$  is the effective mass of the carriers, and  $v$  is the velocity component perpendicular to the magnetic field. The fundamental quantity for MR is  $\omega_c\tau$ , the mean angle turned along the helical path between collisions, where  $\omega_c = eB/m^*c$  is the cyclotron frequency. In the as-deposited polycrystalline Bi films with a shorter  $l$ , a large fraction of scattering events occurs at the grain boundaries, resulting in a smaller relaxation time, hence, a much smaller MR effect. In single-crystalline Bi films, grain boundary scattering is suppressed, as demonstrated by a reduced resistivity value by about a factor of 5 in the single-crystalline films, resulting in a much longer  $l$  (see below) and a larger MR effect.

Because  $l$  in Bi can be very large in high quality samples [12], finite-size effects can be observed in relatively thick films when  $l$  becomes comparable to, or larger than, the film thickness. We have also measured the Hall effect of single-crystalline Bi films. From the Hall coefficient, we obtained the electron density of  $3.66 \times 10^{17} \text{ cm}^{-3}$ , which is in good agreement with those reported for bulk single crystal Bi [23] and epitaxial Bi films [20]. From these results, the value of  $l$  at 5 K for the 5- $\mu\text{m}$  films has been found to be about 4.7  $\mu\text{m}$ . Hence, all of the single-crystalline Bi films studied here are in the regime where finite-size effects are important.

For the perpendicular MR, the cyclotron orbit is in the film plane. Essentially all carriers are in cyclotron motion, thus contribute to the MR. Therefore, the perpendicular MR is always the largest. In contrast, in the longitudinal MR, the cyclotron orbits are perpendicular to the film plane. Because  $\mathbf{B}$  is along the current density, only a small fraction of the carrier motions contributes to the MR. The longitudinal MR is therefore always the smallest. In the transverse geometry, the cyclotron orbital planes are also perpendicular to the film plane, but with  $\mathbf{B}$  perpendicular to the current density, hence, also a large MR. For thick polycrystalline films with small grains, whose sizes are small compared with the film thickness, the transverse MR should approximately be the same as that of the perpendicular MR. Only in thinner polycrystalline films does the transverse MR become significantly less than the perpendicular MR. These features have been observed in polycrystalline films as the thickness is reduced, as shown in Table I. The decrease of the MR ratio with decreasing film thickness in polycrystalline Bi thin films is due in part to the smaller grain size. In polycrystalline Bi films, the average grain size is smaller for thinner films. The grain boundary scattering significantly increases the resistivity value in films with decreasing thickness, as shown in Table I.

As in the polycrystalline films, the longitudinal MR of the single-crystalline films is always the smallest; the perpendicular MR is the largest. However, the difference between the perpendicular and transverse MR is much larger than that in the polycrystalline films because of the finite-size effects, which are important for both MR and resistivity because of the very large values of  $l$  in the single-crystalline Bi films. In thin films, the carriers experience scattering from the film surfaces. In the thin film limit  $t \ll l$ , the ratio of resistivities of the film ( $\rho_F$ ) and bulk ( $\rho_B$ ) varies as  $\rho_F/\rho_B = 4[\ln(1/\gamma) + 0.423]/3\gamma$ , where  $\gamma = t/l$  [24]. As a result, the resistivity of the single-crystalline Bi film increases with decreasing thickness, from 34  $\mu\Omega \text{ cm}$  for the 10- $\mu\text{m}$  film to 78  $\mu\Omega \text{ cm}$  for the 1- $\mu\text{m}$  film.

The MR ratios of the annealed single-crystalline Bi films decrease with decreasing film thickness  $t$ . In thinner films, surface scattering is more severe. Carrier mean free path  $l$  and relaxation time  $\tau$  are effectively reduced due to the surface scattering. As the cyclotron frequency  $\omega_c$  is independent of the film thickness, the fundamental quantity  $\omega_c\tau$ , and consequently the MR ratios, decreases with decreasing thickness.

In the perpendicular geometry, the cyclotron orbits of carriers are mainly parallel to the film plane, thus less affected by the surfaces. The effective  $\omega_c\tau$  is close to that of bulk material, hence, a very large MR. In the transverse geometry, the cyclotron orbits of electrons are perpendicular to the film. The radius of the cyclotron orbits decreases with increase of magnetic field. The carriers, moving further away from the surfaces, receive less scattering from the surfaces. The ratio  $\rho_F/\rho_B$  decreases with increasing  $H$  and approaches 1 in very high fields. Thus the transverse MR is considerably smaller than the perpendicular MR. The difference between the perpendicular and transverse MR becomes smaller for thicker films, as indeed is observed in Table I.

While the field dependence of the MR in Bi is quasilinear, such as those shown in Fig. 2a, the MR results of the single-crystalline Bi films shown in Fig. 2c exhibit distinct oscillations superimposed on the quasilinear field dependence. These are the Shubnikov-de Haas (SdH) oscillations, which can be more clearly shown by subtracting the quasilinear background, as shown in Fig. 3a. The resistivity minima at 1.4, 2.2, and 3.9 T are taken as the locations of the SdH oscillations. The Fermi surface of Bi consists of three ellipsoidal electron surfaces symmetrical about, and one hole surface along, the trigonal axis. In the perpendicular geometry, the SdH oscillations originate from the hole surface along the trigonal axis. Comparing with the results in single-crystal Bi [25], we found that the minimum at 3.9 T is due to the hole Landau level of  $2^-$ , and the minima at 2.2 T is due to the levels of  $1^+$  and  $3^-$  which are overlapping, where + and - denote spin directions. The minimum at 1.4 T is from higher Landau levels. These minima are periodic with  $1/H$  as shown in Fig. 3b.

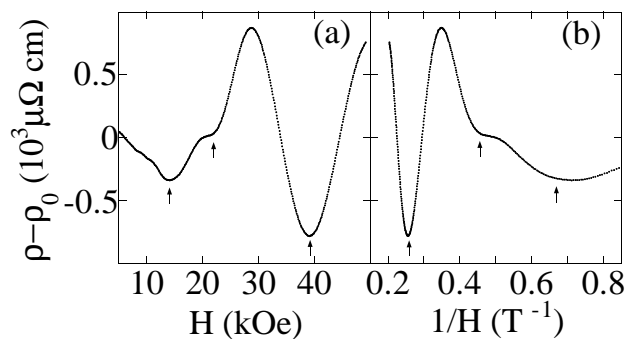


FIG. 3. Shubnikov-de Haas oscillations for a magnetic field applied perpendicular to the film plane and along the trigonal axis of a 10- $\mu\text{m}$  single-crystalline Bi film plotted as (a)  $\rho - \rho_0$  vs  $H$  and (b)  $\rho - \rho_0$  vs  $1/H$ . The background resistivity  $\rho_0(H)$  is obtained from a quasilinear fit: quadratic at small field and linear at large field. The arrows point to the oscillation positions.

Also of interest, particularly for technological applications, is the MR effect at room temperature. As expected, the MR effect at room temperature is much smaller because of a much smaller  $\omega_c\tau$ . While the MR effect at low temperatures depends on the quality of the sample (polycrystalline vs single crystalline) and film thickness, the MR ratio at room temperature is roughly the same for all of the films studied within the thickness range of 1–10  $\mu\text{m}$ . The MR ratio of the 10- $\mu\text{m}$  Bi film at room temperature is 2.4 for polycrystalline and 2.9 for single crystalline, which is still much larger than the largest GMR values reported for magnetic nanostructures at any temperature. The nonhysteretic MR of the Bi films, increasing unabatedly with field with a prescribed dependence, can be used for wide-range field and current sensors. The intrinsic GMR effect in magnetic nanostructures occurs only at large magnetic fields [1,2]. It is the advent of spin-valve and other structures that allows the GMR effect to be useful for detecting small magnetic fields. The intrinsic positive MR effect in Bi films is even larger. Using hybrid structures incorporating Bi thin films, the large MR effect in Bi can also be utilized to detect smaller magnetic fields. Such explorations are underway.

In summary, using electrodeposition in conjunction with processing, we have successfully fabricated high quality Bi thin films, which exhibit a very large MR effect and Shubnikov-de Haas oscillations. These Bi thin films can be used to study finite-size effects of the fascinating transport properties and for technological applications.

This work has been supported by NSF Grants No. DMR96-32526 and No. DMR97-32763.

- [1] M.N. Baibich, J.M. Broto, A. Fert, F. Nguyen van Dau, F. Petroff, P. Etienne, G. Creuzet, A. Friederich, and J. Chazeles, *Phys. Rev. Lett.* **61**, 2472 (1988).
- [2] S.S.P. Parkin, R. Bhadra, and K.P. Roche, *Phys. Rev. Lett.* **66**, 2152 (1991).
- [3] B. Dieny, V.S. Speriosu, S. Metin, S.S.P. Parkin, B.A. Gurney, P. Baumgart, and D.R. Wilhoit, *J. Appl. Phys.* **69**, 4774 (1991).
- [4] A.E. Berkowitz, J.R. Mitchell, M.J. Carey, A.P. Young, S. Zhang, F.S. Spada, F.T. Parker, A. Hutten, and G. Thomas, *Phys. Rev. Lett.* **68**, 3745 (1992).
- [5] J.Q. Xiao, J.S. Jiang, and C.L. Chien, *Phys. Rev. Lett.* **68**, 3749 (1992).
- [6] P. Grünberg, R. Schreiber, Y. Pang, M.B. Brodsky, and H. Sowers, *Phys. Rev. Lett.* **57**, 2442 (1986).
- [7] E.E. Fullerton, M.J. Conover, J.E. Mattson, C.H. Sowers, and S.D. Bader, *Appl. Phys. Lett.* **63**, 1699 (1993); *Phys. Rev. B* **48**, 15755 (1993).
- [8] H. Kano, K. Kagawa, A. Suzuki, A. Okabe, K. Hayashi, and K. Aso, *Appl. Phys. Lett.* **63**, 2839 (1993).
- [9] R. von Helmolt, J. Wecker, B. Holzapfel, L. Schultz, and K. Samwer, *Phys. Rev. Lett.* **71**, 2331 (1993).
- [10] S. Jin, T.H. Tiefel, M. McCormack, R.A. Fastnacht, R. Ramesh, and L.H. Chen, *Science* **264**, 413 (1994).
- [11] N. Garcia, Y.H. Kao, and M. Strongin, *Phys. Rev. B* **5**, 2029 (1972).
- [12] D.H. Reneker, *Phys. Rev. Lett.* **1**, 440 (1958); W.S. Boyle and G.E. Smith, *Prog. Semicond.* **7**, 1 (1963).
- [13] Yu.F. Komnik, E.I. Bukhshab, Yu.V. Nikitin, and V.V. Andrievskii, *Zh. Eksp. Teor. Fiz.* **60**, 669 (1971) [*Sov. Phys. JETP* **33**, 364 (1971)].
- [14] C.A. Hoffmann, J.R. Meyer, F.J. Bartoli, A. Di Venere, X.J. Yi, C.L. Hou, H.C. Wang, J.B. Ketterson, and G.K. Wong, *Phys. Rev. B* **48**, 11431 (1993).
- [15] M. Lu, R.J. Zieve, A. van Hulst, H.M. Jaeger, T.F. Rosenbaum, and S. Radelaar, *Phys. Rev. B* **53**, 1609 (1996).
- [16] J.H. Mangez, J.-P. Issi, and J. Heremans, *Phys. Rev. B* **14**, 4381 (1976).
- [17] P.B. Alers and R.T. Webber, *Phys. Rev.* **91**, 1060 (1953).
- [18] D.E. Beutler and N. Giordano, *Phys. Rev. B* **38**, 8 (1988).
- [19] T. Missana and C.N. Afonso, *Appl. Phys. A* **62**, 513 (1996).
- [20] D.L. Partin, J. Heremans, D.T. Morelli, C.M. Thrush, C.H. Olk, and T.A. Perry, *Phys. Rev. B* **38**, 3818 (1988).
- [21] Kai Liu, C.L. Chien, P.C. Searson, and Kui Yu-Zhang, *Appl. Phys. Lett.* **73**, 1436 (1998).
- [22] Kai Liu, C.L. Chien, and P.C. Searson, *Phys. Rev. B* **58**, R14681 (1998).
- [23] G.E. Smith, G.A. Baraff, and J.M. Rowell, *Phys. Rev.* **135**, A1118 (1964).
- [24] K. Fuchs, *Proc. Cambridge Philos. Soc.* **34**, 100 (1938); E.H. Sondheimer, *Adv. Phys.* **1**, 1 (1952).
- [25] Kenji Hiruma and Noboru Miura, *J. Phys. Soc. Jpn.* **52**, 2118 (1983).